Conformational properties of bottle-brush polymers

N. A. Denesyuk*
Department of Chemistry, University of Cambridge, Lensfield Road, Cambridge CB2 1EW, United Kingdom
(Received 17 March 2002; revised manuscript received 18 December 2002; published 27 May 2003)

General and renormalized perturbation theories are used to study the conformational properties of a bottle-brush molecule, composed of multiarmed polymer stars grafted regularly onto a flexible backbone. The end-to-end distances of the backbone and of an arm of the middle star are calculated within the first order of perturbation theory. For the high grafting densities of stars, the calculated expressions are generalized with the help of the scaling arguments to give the equivalent power laws. According to these laws, the molecule may adopt a sequence of three different conformations (star-rod-coil) as the length of the backbone grows.

DOI: 10.1103/PhysRevE.67.051803 PACS number(s): 61.41.+e, 81.05.Lg

I. INTRODUCTION

Cylindrical comb copolymer brushes, or bottle-brush molecules, have been attracting much experimental [1–8] and computational [9–14] attention. Such molecules consist of a flexible backbone grafted densely with either flexible or rigid side chains. The high grafting density of side chains implies that the number of the backbone segments L, confined between the adjacent points of grafting, is much smaller than the degree of polymerization N of a side chain. In the presence of excluded volume interactions, the grafted chains try to avoid strong overlapping, which induces a significant increase in the stiffness of the backbone. As a result, the bottle-brush molecule can be found in three different conformational states depending on the backbone's molecular weight.

If the size of the backbone is much smaller than that of a side chain, the bottle-brush molecule effectively represents a star, in which the number of arms is equal to the total number of the grafted chains. As the length of the backbone grows, but remains smaller than a certain crossover value, the shape of the molecule changes gradually from a sphere into a stiff cylinder. The radius of such a cylinder is given by the size of the grafted chains, while its length grows proportionally to the backbone's molecular weight. Finally, when the size of the backbone is sufficiently large, the grafted chains are no longer a restriction on the backbone's folding and it adopts a highly swollen coil-like conformation. We should note that such a rich conformational behavior can only be observed at high grafting densities of the side chains, i.e., when $L \ll N$. For $L \sim N$ the backbone chain always remains flexible and only slightly extended due to the excluded volume interactions of the side chains.

The cylindrical conformations of the bottle-brush molecules have been studied in detail within a self-consistent field approach [15–17]. In this analysis, the backbone is modeled as a semiflexible chain characterized by its persistence and contour lengths. The grafting of side chains increases the original persistence length of the backbone, and this increase can be determined by comparing the free energies of the fully stretched and the slightly bent brushes [15,16]. With regard to the conformational properties of the side chains, the numerical self-consistent field calculation [17] as well as the simple variational approach [18], provide the two-dimensional exponent $\nu = 3/4$ (characteristic of a cylindrical conformation) in the power law dependence between the size of a side chain and its length. This corresponds to the physical situation where each side chain is confined to a narrow disk created by the neighboring chains and can wander only in directions perpendicular to the backbone. Computer simulations [9,10,14] show, however, that the size of a side chain obeys the scaling law with the three-dimensional exponent $\nu = 3/5$ (characteristic of a star conformation), although some authors [11–13] report slightly larger values of ν. This suggests that the side chains are found at the crossover between their three-dimensional and quasi-two-dimensional configurations. Therefore, in the present work, we go beyond the self-consistent field analysis and study the complete conformational behavior of the comb copolymer brushes.

We consider a bottle-brush molecule with a fully flexible backbone and side chains of the same chemical composition, placed in a very good solvent so that the excluded volume correlations are significant. The number of side chains, f, attached to each point of branching is taken to be arbitrary, i.e., $f \geqslant 1$. We treat such a system within *renormalized* perturbation theory as discussed in Ref. [19] (see Appendix A for a brief summary). In the following sections we construct a first-order perturbation theory for the end-to-end distance of the backbone and of a central side chain in the bottle-brush molecule. This perturbation theory is then renormalized in order to remove the divergencies caused by the high degrees of polymerization of the linear chains. The calculated first-order corrections depend on the grafting density of the side chains and parameter f and remain small for the sufficiently low values of these parameters. In this case, the first-order corrections give the correct estimates of the additional swelling of the linear chains comprising the molecule, which is due to the mutual connectivity of these chains. However, when parameters N/L and f are large, the calculated expressions diverge and cannot be used directly to estimate the examined end-to-end distances. At this point, we employ the scaling arguments to transform the first-order corrections into equivalent power laws.

A discussion of the resulting scaling relationships and crossovers between them is contained in Secs. III D, IV, and

*Electronic address: nad28@cam.ac.uk

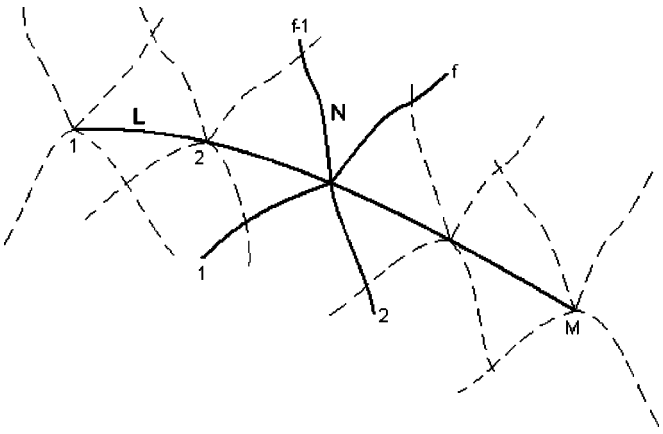

FIG. 1. Schematic representation of a bottle-brush molecule studied in this paper.

V. In addition, in Sec. V we present a scaling argument to obtain the persistence length of a long bottle-brush molecule and compare our result with other predictions of the same quantity [15,20,21].

II. DESCRIPTION OF THE MODEL

In this work a bottle-brush molecule is modeled by M stars, each containing f flexible chains of length N, grafted regularly with intervals of L segments onto a flexible backbone of length $L(M-1)$ (see Fig. 1). Since we assume the presence of excluded volume correlations, we apply the model of a self-repelling Gaussian chain to describe each of the linear chains comprising the molecule (one backbone and fM side chains). The partition function of the entire molecule takes the form

$$Z=\int D[\mathbf{r}]\exp[-V(\mathbf{r}_{\{i,k\}})], \tag{1}$$

where subscript i labels polymer segments within the linear chain k. In Eq. (1) we denote

$$D[\mathbf{r}]=\prod_{i=0}^{L(M-1)}\frac{d\mathbf{r}_{\{i,0\}}}{(4\pi l^2)^{d/2}}\prod_{k=1}^{fM}\prod_{i=0}^{N}\frac{d\mathbf{r}_{\{i,k\}}}{(4\pi l^2)^{d/2}} \tag{2}$$

and

$$\exp(-V)=\prod_{i_1k_1,i_2k_2}[1-(4\pi l^2)^{d/2}\beta_e\delta(\mathbf{r}_{\{i_1,k_1\}}-\mathbf{r}_{\{i_2,k_2\}})]\times\exp\left(-\frac{1}{4l^2}\sum_{i=1}^{L(M-1)}(\mathbf{r}_{\{i,0\}}-\mathbf{r}_{\{i-1,0\}})^2-\frac{1}{4l^2}\sum_{k=1}^{fM}\sum_{i=1}^{N}(\mathbf{r}_{\{i,k\}}-\mathbf{r}_{\{i-1,k\}})^2\right). \tag{3}$$

Parameters l and β_e stand for the segment size and excluded volume, respectively, whereas d is the spatial dimension. We can now introduce the pair correlation function $P(\mathbf{r},\{i_1,k_1\},\{i_2,k_2\})$, which describes the probability of two segments $\{i_1,k_1\}$ and $\{i_2,k_2\}$ being separated by a distance $\mathbf{r}$. We will be concerned with the Fourier transform of $P(\mathbf{r},\{i_1,k_1\},\{i_2,k_2\})$,

$$P(\mathbf{q},\{i_1,k_1\},\{i_2,k_2\})=\frac{1}{Z}\int D[\mathbf{r}]\exp[i\mathbf{q}\cdot(\mathbf{r}_{\{i_1,k_1\}}-\mathbf{r}_{\{i_2,k_2\}})]\exp(-V). \tag{4}$$

The function $P(\mathbf{q})$ is often used to calculate the mean-squared distance R^2 between the labeled segments,

$$R^2=-2d\frac{\partial}{\partial\mathbf{q}^2}P(\mathbf{q})|_{\mathbf{q}=0}. \tag{5}$$

A specific choice of $\{i_1,k_1\}$ and $\{i_2,k_2\}$ defines the scale on which the molecule is considered. In the two interesting cases, $\{i_1=0,k_1\neq 0\}$, $\{i_2=N,k_2=k_1\}$ and $\{i_1=0,k_1=0\}$, $\{i_2=L(M-1),k_2=0\}$, Eq. (5) provides estimates R_t and R_l for the diameter and the extent of a bottle-brush molecule. As a starting point, we calculate these quantities by expanding Eqs. (4) and (5) to the first order in powers of β_e. Each term in such an expansion can be depicted as a diagram and can be calculated using the Feynman rules. We will first consider R_t to illustrate the method.

III. GENERAL AND RENORMALIZED PERTURBATION THEORIES FOR THE END-TO-END DISTANCE OF A SIDE CHAIN

A. The Feynman rules

Let $G(\mathbf{q})$ denote the path integral in Eq. (4),

$$G(\mathbf{q},\{i_1,k_1\},\{i_2,k_2\})=\int D[\mathbf{r}]\exp[i\mathbf{q}\cdot(\mathbf{r}_{\{i_1,k_1\}}-\mathbf{r}_{\{i_2,k_2\}})]\exp(-V). \tag{6}$$

Then Eq. (4) can be rewritten in the form

$$P(\mathbf{q},\{i_1,k_1\},\{i_2,k_2\})=\frac{G(\mathbf{q},\{i_1,k_1\},\{i_2,k_2\})}{G(\mathbf{0},\{i_1,k_1\},\{i_2,k_2\})}. \tag{7}$$

If the perturbation series for $G(\mathbf{q})$ is known,

$$G(\mathbf{q})=G_0(\mathbf{q})+\beta_eG_1(\mathbf{q})+O(\beta_e^2), \tag{8}$$

it can also be defined for the function $P(\mathbf{q})$,

$$P(\mathbf{q})=\frac{G_0(\mathbf{q})}{G_0(\mathbf{0})}+\beta_e\left(\frac{G_1(\mathbf{q})}{G_0(\mathbf{0})}-\frac{G_0(\mathbf{q})G_1(\mathbf{0})}{G_0^2(\mathbf{0})}\right)+O(\beta_e^2)=P_0(\mathbf{q})+\beta_e\left(\frac{G_1(\mathbf{q})}{G_0(\mathbf{0})}-P_0(\mathbf{q})\frac{G_1(\mathbf{0})}{G_0(\mathbf{0})}\right)+O(\beta_e^2). \tag{9}$$

Here $P_0(\mathbf{q})$ is the end point distribution of an ideal chain,

$$P_0(\mathbf{q},n)=\exp(-\mathbf{q}^2l^2n), \tag{10}$$

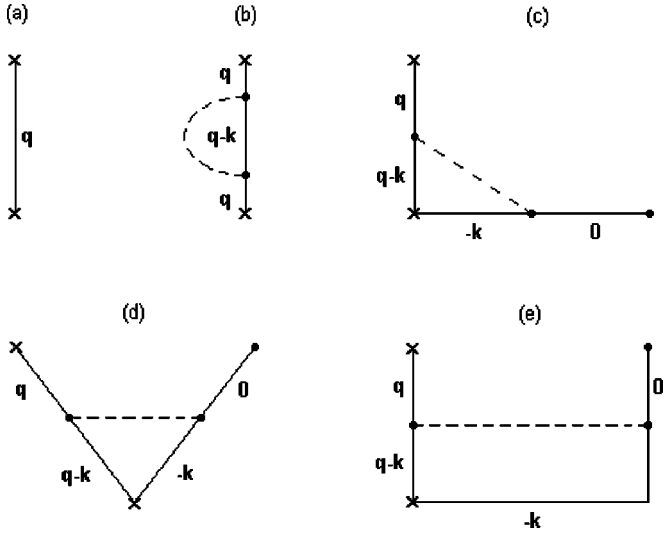

FIG. 2. Diagrammatic representations of the zero-order D_0 (a) and the first-order D_1 (b), D_2 (c), D_3 (d), D_4 (e) corrections to the end-to-end distribution of a side chain.

n being the chain length. Diagrammatic representations of functions $G_0(\mathbf{q},\{0,k_1\},\{N,k_1\})$ and $\beta_e G_1(\mathbf{q},\{0,k_1\},\{N,k_1\})$ are shown in Fig. 2 [note that we do not include the diagrams that give a zero contribution to Eq. (9)]. In Fig. 2 the polymer is depicted by a solid line, while broken lines connect the interacting segments. Every diagram contains special points of different types, namely, segments $\{0,k_1\}$ and $\{N,k_1\}$ marked with crosses, as well as interacting segments, points of branching and free ends marked with dots. A solid line connecting two special points is called a propagator, and each diagram contains only those propagators that affect its value. The calculation is performed according to the general Feynman rules constructed for systems of linear chains. The main peculiarity of the present system is the existence of branching points whose effect is identical to that of the interacting segments. Following the Feynman rules, we attach a certain momentum variable to each propagator line respecting momentum conservation throughout. Segments $\{0,k_1\}$ and $\{N,k_1\}$ carry additional external momenta $\mathbf{q}$ and $-\mathbf{q}$, while the external momenta of free ends equal zero. Each propagator of length n and momentum $\mathbf{k}$ produces a factor of $P_0(\mathbf{k},n)$; a broken line yields an additional factor of $-(4\pi l^2)^{d/2}\beta_e$. To obtain the final value of a diagram we need to integrate over all internal momenta $\int d^dk/(2\pi)^d$, then sum over variable side chains and points of interaction and finally multiply the result by an overall factor of $\Omega/(4\pi l^2)^{d/2}$, Ω being the system volume.

B. General perturbation theory

Let us now look at the physical meaning of the diagrams shown in Fig. 2. The simplest diagram D_0 of Fig. 2(a) contains no broken lines and stands for the ideal approximation $P_0(\mathbf{q})$ to the end-to-end distribution $P(\mathbf{q})$. In turn, all diagrams in Figs. 2(b)–2(e) contain a single broken line and represent different interactions of chain k_1. Thus, diagram D_1 incorporates the interactions of chain k_1 with itself; we note that a single interacting polymer chain has been studied in detail elsewhere [22–24]. D_2 takes account of the interactions with the backbone that causes some additional swelling of the chain k_1. The corresponding swelling factor depends on the lengths of both chains, as well as the position of the side chain along the backbone, but always remains of order 1. Diagram D_3 presents the interactions of chain k_1 with other chains within the same star, and its value is proportional to $f-1$. It does not depend on the parameter $\alpha = L/N$ that defines the grafting density of stars in the bottle-brush molecule. Finally, diagram D_4 allows for the interactions of a given side chain with chains belonging to other stars and has a dominant value in the case of high grafting density (small α). In this limit, D_4 is proportional to the ratio f/α (see below) that plays an important role in the scaling properties of a bottle-brush molecule.

With this physical interpretation, we can express the end-to-end distribution $P(\mathbf{q})$ in the form

$$P(\mathbf{q},\{0,k_1\},\{N,k_1\}) = P_0(\mathbf{q},N)\{1-\beta_e N^{\varepsilon/2}[D_1(Q) + D_2(Q,\alpha,m_1,M) + D_3(Q,f) + D_4(Q,f,\alpha,m_1,M)] + O(\beta_e^2)\}, \tag{11}$$

where new designations $Q=\mathbf{q}^2 l^2 N$ and $\varepsilon = 4-d$ are introduced; parameter m_1 denotes the star that contains chain k_1,

$$k_1 \in [f(m_1-1)+1, fm_1].$$

The detailed expressions for $D_i(\mathbf{q})$ are given in Appendix B. Functions $D_i(\mathbf{q})$ appear to change very slightly for different values of m_1, and we conclude that the physical properties of all side chains are roughly the same. We will, therefore, concentrate our attention on a chain belonging to the central star, which is characterized by $m_1=(M+1)/2$. The corresponding expressions for the end-to-end distance R_t of such a chain, obtained from Eqs. (11) and (5), are also included in Appendix B.

C. Renormalized perturbation theory

At this stage we apply the renormalization group techniques, sketched in Appendix A, to transform the end-to-end distance R_t of a central side chain into the strict ε expansion. We simply express Eq. (B2) of Appendix B in terms of the renormalized parameters l_R, n_R, $u=u^*$ and expand the result to the first order in powers of ε. We get

$$R_t^2 = 2dl_R^2 n_R\left[1+\frac{\varepsilon}{8}(\overline{R}_1+\overline{R}_2+\overline{R}_3+\overline{R}_4)+O(\varepsilon^2)\right], \tag{12}$$

where

$$\overline{R}_1 = \ln n_R - 1,\ \ \overline{R}_2 = R_2|_{d=4} = h(X),$$

$$\overline{R}_3 = R_3|_{d=4} = (f-1)\left(\ln 2 - \frac{1}{4}\right),$$

$$\overline{R_4}=R_4|_{d=4}=\frac{2f}{c-1}\int_0^{c-1}dzz[\Psi(\overline{M}+1+z)-\Psi(\overline{M}+c+z)+\Psi(c+z)-\Psi(1+z)]+f(c-1)\times[\Psi(\overline{M}+2c-1)-\Psi(\overline{M}+c)+\Psi(c)-\Psi(2c-1)]$$

and

$$h(X)=2X\ln\left(1+\frac{1}{X}\right)-\frac{X}{X+1},$$

$$c=1+\frac{1}{\alpha},\quad \overline{M}=\frac{M-1}{2},\quad X=\alpha\overline{M},\quad \Psi(z)=\frac{d\ln\Gamma(z)}{dz}.$$

It is appropriate to consider the ratio R_t/R_{t0}, where R_{t0} is the end-to-end distance of a given side chain when it is not connected to other chains. In this case, the renormalized degree of polymerization n_R drops out from Eq. (12) and we have

$$\frac{R_t^2}{R_{t0}^2}=1+\frac{\varepsilon}{8}(\overline{R}_2+\overline{R}_3+\overline{R}_4)+O(\varepsilon^2). \tag{13}$$

The maximum value of the first-order correction, given by Eq. (13), is essentially determined by two parameters, c and f. For the low grafting densities of side chains, described by the fairly small values of c and f, the first-order correction remains smaller than 1 (we take $\varepsilon=1$ for $d=3$). In this case, Eq. (13) can be used directly to estimate the additional swelling of a central side chain due to its interactions with other chains in the molecule. We would like to note that, in the particular case of $f=1$, the first-order correction stays quantitatively valid up to $c\simeq 10$. When parameters c and f are large, Eq. (13) becomes quantitatively irrelevant but can be modified to give a few helpful results.

To conclude this section we note that, ultimately, we are interested in the limit of high grafting densities $\alpha\ll 1$ (or $c\gg 1$), when the bottle-brush molecule shows its rich conformational behavior. In this limit, the expression for $\overline{R}_4$ can be noticeably simplified if we substitute the function $\Psi(z)$ with its asymptotic expression,

$$\Psi(z)=\ln(z)-\frac{1}{2z}+O\left(\frac{1}{z^2}\right),$$

and expand the result in powers of α. We find

$$\overline{R}_4=f\left(\frac{h_1(X)}{\alpha}+h_2(X)+O(\alpha)\right), \tag{14}$$

where

$$h_1(X)=(X+1)^2\ln\left(1+\frac{1}{X+1}\right)-X^2\ln\left(1+\frac{1}{X}\right)-\ln 2,$$

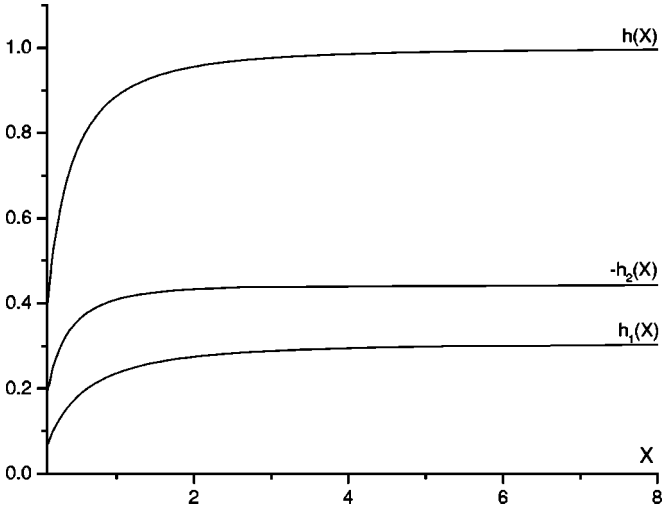

FIG. 3. Functions $h_1(X)$, $h_2(X)$, and $h(X)$ of Sec. III C.

$$h_2(X)=(X+1)\ln\left(1+\frac{1}{X+1}\right)-X\ln\left(1+\frac{1}{X}\right)-\ln 2+\frac{1}{4}\frac{X(X+3)}{(X+1)(X+2)}.$$

Substituting Eq. (14) back into Eq. (13) yields

$$\frac{R_t^2}{R_{t0}^2}=1+\frac{\varepsilon}{8}\left[\frac{f}{\alpha}h_1(X)+fh_2(X)+(f-1)\left(\ln 2-\frac{1}{4}\right)+h(X)\right]+O(\varepsilon^2,\alpha\varepsilon). \tag{15}$$

We shall now analyze Eq. (15) in more detail.

D. Scaling theory in the limit of high grafting densities

A distinct property of the first-order correction, given by Eq. (15), is its dependence on the number of stars M only via parameter $X\sim\alpha M$. Functions $h_1(X)$, $h_2(X)$, and $h(X)$ exhibit a crossover between two limiting cases $X\ll 1$ and $X\gg 1$ (see Fig. 3) that correspond to the two scaling limits in the behavior of R_t. If the chains comprising a bottle-brush molecule are ideal, condition $X\ll 1$ implies that the size of the backbone is negligibly small,

$$\frac{R_l}{R_t}\sim\frac{(LM)^{1/2}}{N^{1/2}}\sim X^{1/2}\ll 1.$$

In the limit $X\to 0$, we have

$$\frac{h_1(X)}{\alpha}\to\frac{2(\ln 2-1/4)X}{\alpha}=(\ln 2-1/4)(M-1),$$

$$h_2(X)\to 0,\quad h(X)\to 0,$$

and, therefore,

$$\frac{R_t^2}{R_{t0}^2}=1+\frac{\varepsilon}{8}(fM-1)\left(\ln 2-\frac{1}{4}\right)+O(\varepsilon^2). \tag{16}$$

Equation (16) reproduces the equivalent result for the end-to-end distance R_t^* of a linear chain, which belongs to a polymer star comprised of fM such chains (cf. the expression for $\overline{R_3}$). The physical interpretation of this result is as follows: when the size of the backbone is much smaller than that of a side chain, all fM chains in a bottle-brush molecule are grafted virtually onto the same point and the molecule appears to be a star. For X small but finite, we can express the end-to-end distance R_t in the form

$$R_t=\kappa R_t^*, \tag{17}$$

where

$$\kappa^2=1+\frac{\varepsilon}{8}\left[\frac{f}{\alpha}\left(h_1(X)-2\left\{\ln 2-\frac{1}{4}\right\}X\right)+fh_2(X)+h(X)\right]+O(\varepsilon^2). \tag{18}$$

When the total number of the grafted stars M is large, the term proportional to f/α in Eq. (18) is dominant. We should note that, in the examined case of high grafting densities $\alpha \ll 1$, conditions $X\sim\alpha M\ll 1$ and $M\gg 1$ are compatible.

The opposite limit $X\gg 1$ corresponds to the backbone sizes R_l that are substantially larger than the size of a side chain R_t. Figure 3 shows that all functions, $h_1(X)$, $h_2(X)$, and $h(X)$, saturate in this limit. This suggests that, in the case of $R_l\gg R_t$, the properties of the side chains are determined locally: two chains will have a noticeable effect on each other only if they appear to be in a constant contact. Let M_s denote the total number of stars that are grafted within the reach of the side chains belonging to the central star, characterized by $m_1=(M+1)/2$. In the ideal bottle-brush molecule, the value of M_s can be determined from the condition

$$\left(\frac{L(M_s-1)}{2}\right)^{1/2}\simeq 2N^{1/2},$$

which yields

$$M_s\simeq\frac{8}{\alpha},\quad X_s\simeq 4. \tag{19}$$

Equation (19) provides a very good estimate for the crossover value X_s (see Fig. 3). Hence, we can rewrite Eq. (15) in terms of parameters f and M_s,

$$\frac{R_t^2}{R_{t0}^2}=1+\frac{\varepsilon}{8}fM_s\overline{h_1}\left(\frac{M}{M_s}\right)+O(\varepsilon^2), \tag{20}$$

where functions h_1 and $\overline{h_1}$ are essentially the same. Note that in Eq. (20) only the dominant contribution, proportional to f/α, is included. We now make an assumption that the sum of the whole series in Eq. (20) has the form

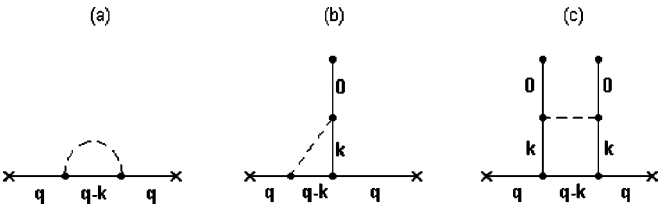

FIG. 4. Diagrammatic representations of the first-order corrections D_1 (a), D_2 (b), D_3 (c) to the end-to-end distribution of the backbone.

$$\frac{R_t}{R_{t0}}=(fM_s)^{1/5}g\left(\frac{M}{M_s}\right), \tag{21}$$

where

$$g(X)\sim\begin{cases}X^{1/5}, & X\ll 1\\ \text{const}, & X\gg 1.\end{cases}$$

The value of the exponent in Eq. (21) has been chosen, in the limit $M\ll M_s$, to reproduce the Daoud-Cotton scaling relationship for a star containing fM branches [25],

$$\frac{R_t}{R_{t0}}\sim(fM)^{1/5}. \tag{22}$$

In the other limit $M\gg M_s$, Eq. (21) yields

$$R_t^{max}\sim(fM_s)^{1/5}N^{3/5}. \tag{23}$$

When we take into account the higher-order terms in Eq. (20), the value of M_s is expected to be different from that given by Eq. (19) and should obey the generalized condition,

$$R_t^{max}\sim R_l(M_s). \tag{24}$$

Here $R_l(M_s)$ denotes the size of the backbone in a bottle-brush molecule, which includes $M=M_s$ stars. In the following sections we calculate the backbone size $R_l(M)$ and present the final results for the quantities M_s and R_t^{max}.

IV. END-TO-END DISTANCE OF THE BACKBONE CHAIN

The calculation of the backbone size R_l is largely based on the material of the preceding section. Thus, the end-to-end distribution $P(\mathbf{q})$ can be written down in full analogy with Eq. (11),

$$P(\mathbf{q},\{0,0\},\{L(M-1),0\})=P_0(\mathbf{q},L(M-1))\{1-\beta_e N^{\varepsilon/2}[D_1(Q)+D_2(Q,f,\alpha,M)+D_3(Q,f,\alpha,M)]+O(\beta_e^2)\}, \tag{25}$$

where individual contributions $D_i(\mathbf{q})$ are depicted in Fig. 4. The diagrams in Fig. 4 allow for different interaction effects such as interactions of the backbone chain with itself (D_1), interactions of the backbone chain with the side chains (D_2), and interactions of the side chains among themselves (D_3). The complete expressions for quantities

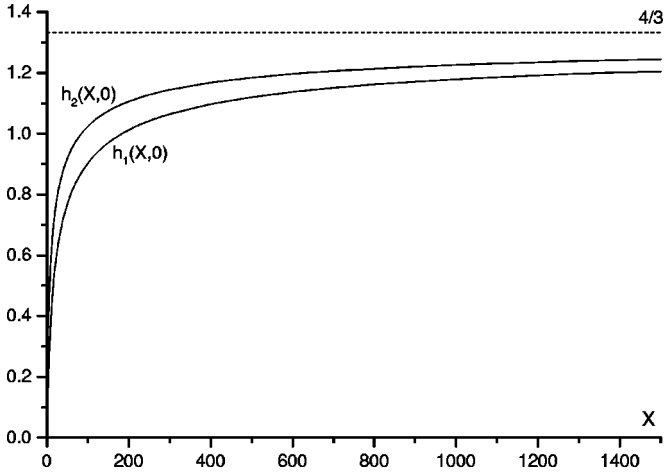

FIG. 5. Functions $h_1(X,\alpha)$ and $h_2(X,\alpha)$ of Sec. IV in the limit of high grafting densities $\alpha \to 0$.

$P(\mathbf{q})$ and R_l are collected in Appendix C. In particular, in the limit of high grafting densities $\alpha \ll 1$, we have

$$\frac{R_l^2}{2dl^2L(M-1)} = 1 + \beta_e (L(M-1))^{\varepsilon/2} \left(\frac{2}{\varepsilon} - \frac{2}{\varepsilon+2} + \frac{f^2}{\alpha^2} h_1(X,\alpha) + 2\frac{f}{\alpha} h_2(X,\alpha) \right) + O(\beta_e^2), \tag{26}$$

where

$$h_1(X,\alpha) = \frac{4}{d(d-2)} X^{-1-\varepsilon/2} \left[\int_0^X dx (X-x) f_1(x) + \alpha \int_0^X dx f_1(x) + o(\alpha) \right],$$

$$h_2(X,\alpha) = \frac{2}{d} X^{-1-\varepsilon/2} \left[\int_0^X dx f_2(x) + o(1) \right], \quad X = \alpha(M-1),$$

and the functions $f_1(x)$ and $f_2(x)$ are interpreted in Appendix C. Similar to Eq. (15) of the preceding section, Eq. (26) shows a crossover between two limiting cases $X \gg 1$ and $X \ll 1$ (see Fig. 5). In the limit $X \gg 1$, the asymptotic behavior of functions h_1 and h_2 is equivalent and independent of α,

$$h_{1,2}(X,\alpha) = \frac{2}{\varepsilon} - \frac{2}{\varepsilon+2} + O(X^{-\varepsilon/2}), \tag{27}$$

which results in

$$\frac{R_l^2}{2dl^2L(M-1)} = 1 + \beta_e \left(1 + \frac{f}{\alpha} \right)^2 [L(M-1)]^{\varepsilon/2} \left(\frac{2}{\varepsilon} - \frac{2}{\varepsilon+2} \right) + O(\beta_e^2). \tag{28}$$

Equation (28) reproduces the result for the end-to-end distance of a linear chain that consists of $n = L(M-1)$ segments, characterized by the excluded volume parameter $\beta_{eff} = \beta_e (1 + f/\alpha)^2$. According to the Flory argument, the end-to-end distance of a polymer chain is given by

$$R(n,\beta_e) \sim \beta_e^{1/5} n^{3/5}, \tag{29}$$

which yields

$$R_l \sim \left(1 + \frac{f}{\alpha} \right)^{2/5} (LM)^{3/5}. \tag{30}$$

We note that, within the renormalization group approach, the situation looks slightly more complicated [19]. Here we should distinguish between $\beta_e < u^*$ (the weak coupling region) and $\beta_e > u^*$ (the strong coupling region), where u^* is defined in Appendix A. In the weak coupling region, we come back to the Flory result for the end-to-end distance of a polymer chain; whereas, in the strong coupling region, Eq. (29) no longer holds and we have instead

$$R(n,\beta_e) \sim \Lambda(\beta_e) n^{3/5},$$

where $\Lambda(\beta_e)$ is some unknown function of β_e. Thus, if the ratio f/α is so large that $\beta_{eff} > u^*$, we should replace Eq. (30) by

$$R_l \sim \Lambda(\beta_e (1 + f/\alpha)^2) (LM)^{3/5}. \tag{31}$$

We would also like to note that, although we assume everywhere $\alpha \ll 1$, the leading asymptotics of functions h_1 and h_2 do not depend on the value of α [see Eq. (27)]. This means that all results obtained in the limit $X \gg 1$ are also valid when the grafting densities of side chains are not high.

In the opposite limit $X \ll 1$, it is convenient to introduce the ratio R_l / R_{l0}, where R_{l0} is the end-to-end distance of the free backbone chain. Since we assume $\alpha \ll 1$, we may consider only the dominant contribution $\sim (f/\alpha)^2$ in Eq. (26), which results in the following ε expansion:

$$\frac{R_l^2}{R_{l0}^2} = 1 + \frac{\varepsilon}{96} [f(M-1)]^2 [1 + O(X)] + O(\varepsilon^2). \tag{32}$$

For small numbers fM of the side chains, the first-order correction in Eq. (32) does not exceed 1. In this case, it can be used directly to estimate the additional swelling of the backbone due to the presence of the grafted chains. If we wish to consider larger molecules, the higher-order terms in Eq. (32) should be taken into account. We suppose that the nth term in Eq. (32) is proportional to $(fM)^{2n}$ and the whole series sums up to give

$$R_l \sim (fM)^{2x} (LM)^{3/5}. \tag{33}$$

The specific value of the exponent x remains undefined in the present approach and has to be borrowed from other theories. If we expect Eq. (33) to describe the stiff rod geometry of a not very long backbone, as has been suggested by numerous experimental works [1–3,6], we should assume $x = 1/5$. Then we have

$$R_l \sim f^{2/5} L^{3/5} M \sim R(L) M, \tag{34}$$

where $R(L)$ denotes the size of a backbone subchain, confined between two adjacent points of grafting. According to Eq. (34), such a subchain is expanded by a factor of $f^{2/5}$ rather than $f^{1/5}$, as it would be if one of its ends were free.

Thus, we can think of a bottle-brush molecule as a worm like chain, characterized by its total length $l_T = R(L)M$ and the persistence length $l_p = R(L)M^*$; here we introduced the crossover parameter M^* such that Eqs. (30) and (34) hold, respectively, for $M > M^*$ and $M < M^*$. Similarly to the results of the preceding section, the crossover behavior of the backbone chain is governed by the parameter $X \sim \alpha M$, and so

$$M^* \sim 1/\alpha. \tag{35}$$

However, the actual value of parameter M^* is much larger than that of M_s (cf. Figs. 3 and 5) and indicates that, in the present case, we are dealing with the global crossover, which involves the molecule as a whole. If we take into account the higher-order terms in the renormalized perturbation theory, Eqs. (19) and (35) cease being valid and we have instead

$$M_s \sim \frac{1}{\alpha}\left(\frac{f}{\alpha}\right)^{\gamma_1}, \quad M^* \sim \frac{1}{\alpha}\left(\frac{f}{\alpha}\right)^{\gamma_2}.$$

The values of exponents γ_1 and γ_2 depend on the exponent x, defined in Eq. (33). In the following section we provide an extra argument in favor of our choice $x = 1/5$ and collect the final results for the end-to-end distances R_t and R_l.

V. DISCUSSION

In order to make the results of the previous sections more complete, let us resort to the simple mean-field analysis. The Flory-type calculation of the dimensions of a bottle-brush molecule, characterized by $f = 1$, is presented in Ref. [26]; here we consider the general case when f is arbitrary. We start with the mean-field expression for the free energy $F(R_t)$, which determines the size of a side chain in the limit of high grafting densities. It reads

$$F(R_t) \sim fM\frac{R_t^2}{N} + \beta_e \frac{(fMN)^2}{R_t^2 R_l}, \tag{36}$$

where we assume that the bottle-brush molecule is found in the rodlike state and, therefore, $R_t \simeq R_t^{max}$ [see Eq. (23)]. Minimizing Eq. (36) with respect to R_t yields

$$R_t^{max} \sim \frac{(fM)^{1/4} N^{3/4}}{R_l^{1/4}}. \tag{37}$$

As shown in the first order of perturbation theory, R_t^{max} does not depend on the number of stars M—a result that seems to be supported by experiment [27]. To satisfy this condition, R_l in Eq. (37) should vary linearly with M, which is consistent with the assumption made on the molecule's geometry and leads to $x = 1/5$ in Eq. (33). Combining Eqs. (34) and (37) we obtain

$$R_t^{max} \sim N^{3/5}\left(\frac{f}{\alpha}\right)^{3/20} \sim N^{3/4} f^{3/20} L^{-3/20}. \tag{38}$$

The dependence of R_t^{max} on the chain length N is described by the two-dimensional exponent $\nu = 3/4$. This reflects the physical situation in which a star is confined to the narrow disk created by the neighboring stars and its branches can wander only in directions perpendicular to the backbone. An alternative way to obtain Eq. (38) is by matching Eqs. (23) and (24), where the backbone size $R_l(M_s)$ is given by Eq. (34). We find

$$M_s \sim \frac{1}{\alpha}\left(\frac{f}{\alpha}\right)^{-1/4}, \tag{39}$$

which together with Eq. (23) brings us back to Eq. (38).

Let us now turn to the properties of a bottle-brush molecule as a whole. If M^* is the number of stars grafted on the molecule's persistence length l_p, then for $M > M^*$ this molecule can be considered as a chain of M/M^* cylindrical segments, each characterized by diameter $d \sim R_t^{max}$ and linear size $l \sim l_p$. The excluded volume of such a segment is $\sim l^2 d$, and we have for the end-to-end distance of a long cylindrical brush

$$R_l \sim d^{1/5} l_p^{1/5} l_T^{3/5}, \tag{40}$$

where l_T stands for the brush's contour length. Taking into account the estimates

$$l_p \sim R(L)M^*, \quad l_T \sim R(L)M,$$

we obtain, from comparing Eqs. (30) and (40),

$$M^* \sim \frac{1}{\alpha}\left(\frac{f}{\alpha}\right)^{1/4}. \tag{41}$$

As expected, the crossover parameters M_s and M^* are given by different scaling relationships of Eqs. (39) and (41). The resulting expression for the persistence length l_p has the form

$$l_p \sim N^{3/5}\left(\frac{f}{\alpha}\right)^{13/20} \sim R_t^{max}\left(\frac{f}{\alpha}\right)^{1/2}. \tag{42}$$

For a simple comb copolymer brush, i.e., a bottle-brush molecule with $f = 1$, we are aware of three other theoretical predictions of the persistence length l_p. According to Birshtein *et al.* [20], persistence length l_p is comparable with brush radius, $l_p \sim R_t^{max}$, while the scaling arguments by Fredrickson [21] show that $l_p \sim R_t^{max} N^{9/8}$. A more recent conclusion of the self-consistent field analysis [15] is that $l_p \sim R_t^{max} N^{5/4}$. The present result corresponds to $l_p \sim R_t^{max} N^{1/2}$ and falls in between these other predictions. We note, however, that the argument we apply to obtain the persistence length l_p of the long bottle-brush molecule is largely based on the assumption that the molecule folds as a self-avoiding cylindrical chain. If we suppose that parts of this chain can

penetrate each other, we would find a larger value of l_p in comparison with that given by Eq. (42).

We now comment on a few interesting properties of the scaling relationships presented here. First of all, from a physical perspective, we expect each star to have an unperturbed three-dimensional core, which comprises the innermost subchains of length N_c and has a radius $R_c \sim f^{1/5} N_c^{3/5}$. Beyond the core region a star should retrieve its global two-dimensional behavior, so that R_c can also be estimated from Eq. (38). On the basis of this observation, we have

$$N_c \sim L f^{1/3},$$

$$R_c \sim L^{3/5} f^{2/5} \sim R(L).$$

We see that the size of the unperturbed zone is determined by the interstar distance $R(L)$, a result consistent with our physical expectations.

Another supporting fact in favor of the present approach is that the scaling relationship of Eq. (30) can also be obtained by the simple mean-field analysis. This amounts to presenting the molecule's free energy as a function of the backbone size R_l,

$$F(R_l) \sim \frac{R_l^2}{LM} + \beta_e \frac{(fMN+LM)^2}{R_l^3},$$

and minimizing it with respect to R_l.

Finally, we would like to note that, in the case of high grafting densities, all the scaling factors that allow for the interactions of the side chains, depend on the single parameter f/α.

VI. CONCLUSION

In this paper, we have investigated the conformational properties of a bottle-brush molecule placed in a very good solvent. We started by calculating the end-to-end distances of the backbone and of a central side chain to the first order of the general and renormalized perturbation theories. The obtained expressions revealed a complex dependence on parameters f and α, where f is the number of side chains attached to each point of branching and α is inversely proportional to the density of such points along the backbone. When $f \sim 1$ and $\alpha \sim 1$, the first-order terms in the renormalized perturbation theory provide a true estimate of the additional swelling of the grafted chains and the backbone. In the opposite limit of high grafting densities $\alpha \ll 1$ and large values of f, the perturbation theory becomes quantitatively invalid but can be generalized to give the correct scaling laws. Naturally, the resulting scaling relationships depend on parameter f only via the ratio f/α. This is the ratio between the total molecular weight fN of the side chains, attached to each point of grafting, and the molecular weight L of a backbone subchain, confined between two neighboring grafting points.

If the grafting density of the side chains is high and constant, the bottle-brush molecule may adopt three different conformations as the size of the backbone grows. When the size of a side chain R_t significantly exceeds the backbone size R_l, the molecule's structure resembles a star in which the number of arms is equal to the total number of side chains fM. In this regime, the side chains are swollen uniformly in all directions and their size is given by the Cotton-Daoud expression of Eq. (22). The first (local) crossover appears when the size of the backbone becomes comparable with that of a side chain, i.e., $R_l \sim R_t$. At this point, the swelling of the side chains drastically slows down and, as the size of the backbone grows further, the bottle-brush molecule starts to resemble a long stiff cylinder. Inside this cylinder, the side chains are swollen in the direction perpendicular to the backbone, and the dependence of the chain's size on its length is defined by the two-dimensional exponent $\nu = 3/4$. The molecule starts to bend when the size of its backbone exceeds the persistence length l_p of the formed cylindrical brush. This marks the second (global) crossover, which describes the configurational changes of the entire cylindrical brush as its internal structure remains unchanged. Ultimately, such a brush should adopt a coiled conformation when the length of the backbone is very large.

ACKNOWLEDGMENT

I am grateful to Professor Jean-Pierre Hansen for introducing me to this problem and for his help in revising the manuscript.

APPENDIX A: BASIC IDEAS OF THE RENORMALIZED PERTURBATION THEORY

In this appendix we present a very short summary of the renormalized perturbation theory as is explained in Ref. [19].

Let us consider a single polymer chain consisting of n segments, each characterized by its linear size l and the excluded volume parameter β_e. It is known that the general perturbation theory for such a system orders in powers of parameter $W = \beta_e n^{\varepsilon/2}$, where

$$\varepsilon = 4 - d$$

and d is the spatial dimension. For chains with a high degree of polymerization n, parameter W is large and the general perturbation theory diverges. The main idea consists in mapping the given polymer chain onto a much shorter one, for which the perturbation theory would be applicable. For this purpose, we perform a spatial dilatation such that the elementary length l transforms according to

$$l \to l_R = l/\lambda, \quad 0 < \lambda < 1. \tag{A1}$$

Since the physical observables should remain invariant upon this transformation, parameters β_e and n should be adjusted accordingly. The dimensional analysis yields

$$\beta_e \to u, \quad \beta_e = \lambda^{\varepsilon} u Z_u(u) \tag{A2}$$

and

$$n \to n_R, \quad n = \lambda^{-2} n_R Z_n(u), \tag{A3}$$

where $Z_u(u)$ and $Z_n(u)$ are the relevant renormalization factors. Within the so-called scheme of ''dimensional regularization'' and ''minimal subtraction'' [19], we have the following expressions for Z_u and Z_n:

$$Z_u(u)=\frac{1}{2}\left(1+\frac{4}{\varepsilon}u+O(u^2)\right), \tag{A4}$$

$$Z_n(u)=1-\frac{1}{\varepsilon}u+O(u^2). \tag{A5}$$

It can be shown that the mapping given by Eqs. (A1)–(A5) justifies the ''fixed point'' hypothesis that states that parameter u approaches some constant value $u=u^*$ as $\lambda\to 0$. The limiting value u^* is known up to the second order in the ε expansion and reads

$$u^*=\frac{\varepsilon}{4}+\frac{21}{128}\varepsilon^2+O(\varepsilon^3). \tag{A6}$$

We can now define the excluded volume limit as a limit that is reached if, under renormalization, parameter u approaches the fixed point so closely that it can be replaced by u^*. Clearly, the excluded volume limit requires the initial degree of polymerization n to be sufficiently high so that λ is close to zero when $n_R\simeq 1$. According to Eqs. (A4)–(A6), in the excluded volume limit the renormalized perturbation theory essentially amounts to expanding in powers of ε. Thus, in the present work we perform all calculations up to the first order in the ε expansion.

APPENDIX B: FIRST-ORDER CORRECTIONS TO THE END-TO-END DISTANCE R_t

In this appendix we present a series of analytical expressions for the end-to-end distance of a side chain. We start with Eq. (11) of the main text and calculate the individual diagrams $D_i(\mathbf{q})$ with the help of the Feynman rules explained within. We obtain

$$P(\mathbf{q},\{0,k_1\},\{N,k_1\}) = P_0(\mathbf{q},N)\left[1-\beta_e N^{\varepsilon/2}\sum_{i=1}^{4} D_i(Q)+O(\beta_e^2)\right], \tag{B1}$$

$$D_1(Q)=\int_0^1 dx_1(1-x_1)x_1^{-d/2}[\exp(Qx_1)-1],$$

$$D_2(Q)=\bar{D}_2(Q,M-m_1)+\bar{D}_2(Q,m_1-1),$$

$$\bar{D}_2(Q,\bar{M})=\int_0^1 dx_1\int_0^{\bar{M}\alpha} dx_2(x_1+x_2)^{-d/2}\times\left[\exp\left(\frac{Qx_1^2}{x_1+x_2}\right)-1\right],$$

$$D_3(Q)=(f-1)\int_0^1 dx_1\int_0^1 dx_2(x_1+x_2)^{-d/2}\times\left[\exp\left(\frac{Qx_1^2}{x_1+x_2}\right)-1\right],$$

$$D_4(Q)=\bar{D}_4(Q,M-m_1)+\bar{D}_4(Q,m_1-1),$$

$$\bar{D}_4(Q,\bar{M})=f\sum_{k=1}^{\bar{M}}\int_0^1 dx_1\int_{k\alpha}^{k\alpha+1} dx_2(x_1+x_2)^{-d/2}\times\left[\exp\left(\frac{Qx_1^2}{x_1+x_2}\right)-1\right],$$

where we have employed the same set of variables as in Eq. (11). Since the scaling properties of all side chains are the same, we will focus our attention on the central star $m_1=(M+1)/2$. In this case combining Eqs. (B1) and (5) yields

$$R_t^2=2dl^2N\left[1+\beta_e N^{\varepsilon/2}\sum_{i=1}^{4} R_i+O(\beta_e^2)\right], \tag{B2}$$

where

$$R_1=\frac{2}{\varepsilon}-\frac{2}{\varepsilon+2},\quad R_2=2\int_0^1 dx_1\int_0^{\bar{M}\alpha} dx_2x_1^2(x_1+x_2)^{-d/2-1},$$

$$R_3=(f-1)\int_0^1 dx_1\int_0^1 dx_2x_1^2(x_1+x_2)^{-d/2-1},$$

$$R_4=2f\sum_{k=1}^{\bar{M}}\int_0^1 dx_1\int_{k\alpha}^{k\alpha+1} dx_2x_1^2(x_1+x_2)^{-d/2-1},$$

and $\bar{M}=(M-1)/2$.

APPENDIX C: FIRST-ORDER CORRECTIONS TO THE END-TO-END DISTANCE R_l

The complete expressions for the end-to-end distribution $P(\mathbf{q})$ of the backbone chain are as follows:

$$P(\mathbf{q},\{0,0\},\{L(M-1),0\}) = P_0(\mathbf{q},L(M-1))\left[1-\beta_e N^{\varepsilon/2}\sum_{i=1}^{3} D_i(Q)+O(\beta_e^2)\right], \tag{C1}$$

where

$$D_1(Q)=[\alpha(M-1)]^{\varepsilon/2}\int_0^1 dx_1(1-x_1)x_1^{-d/2}[\exp(Qx_1)-1],$$

$$D_2(Q)=2f\sum_{k=1}^{M-1}\int_0^{k\alpha}dx_1\int_0^1 dx_2(x_1+x_2)^{-d/2}\times\left[\exp\left(\frac{Qx_1^2}{x_1+x_2}\right)-1\right],$$

$$D_3(Q)=f^2\sum_{k=1}^{M-1}(M-k)\int_0^1 dx_1\int_0^1 dx_2(x_1+x_2+k\alpha)^{-d/2}\times\left[\exp\left(\frac{Qk^2\alpha^2}{x_1+x_2+k\alpha}\right)-1\right].$$

Combining Eqs. (C1) and (5) yields

$$R_l^2=2dl^2L(M-1)\left[1+\beta_e(L(M-1))^{\varepsilon/2}\sum_{i=1}^{3}R_i+O(\beta_e^2)\right], \tag{C2}$$

where

$$R_1=\frac{2}{\varepsilon}-\frac{2}{\varepsilon+2},$$

$$R_2=2f(\alpha(M-1))^{-1-\varepsilon/2}\times\sum_{k=1}^{M-1}\int_0^{k\alpha}dx_1x_1^2\int_0^1 dx_2(x_1+x_2)^{-d/2-1},$$

$$R_3=f^2(\alpha(M-1))^{-1-\varepsilon/2}\times\sum_{k=1}^{M-1}\alpha^2k^2(M-k)\int_0^1 dx_1\int_0^1 dx_2\times(x_1+x_2+k\alpha)^{-d/2-1}.$$

In the case of high grafting densities $\alpha\ll 1$, the sums over k in the above expressions can be substituted by integrals, which leads to Eq. (26) of the main text. We do not rewrite it here but specify functions f_1 and f_2:

$$f_1(x)=x^2[x^{1-d/2}+(2+x)^{1-d/2}-2(1+x)^{1-d/2}],$$

$$f_2(x)=\frac{1}{3-d/2}[x^{3-d/2}+1-(x+1)^{3-d/2}]-\frac{2}{2-d/2}\times[1-(x+1)^{2-d/2}]+\frac{1}{1-d/2}[1-(x+1)^{1-d/2}].$$

[1] Y. Tsukahara, K. Tsutsumi, Y. Yamashita, and S. Shimada, Macromolecules **23**, 5201 (1990).
[2] Y. Tsukahara, S. Kohjiya, K. Tsutsumi, and Y. Okamoto, Macromolecules **27**, 1662 (1994).
[3] Y. Tsukahara, Y. Ohta, and K. Senoo, Polymer **36**, 3413 (1995).
[4] M. Wintermantel, M. Schmidt, Y. Tsukahara, K. Kajiwara, and S. Kohjiya, Macromol. Rapid Commun. **15**, 279 (1994).
[5] M. Wintermantel, M. Gerle, K. Fischer, M. Schmidt, I. Wataoka, H. Urakawa, K. Kajiwara, and Y. Tsukahara, Macromolecules **29**, 978 (1996).
[6] S.A. Prokhorova and S.S. Sheiko, Macromol. Rapid Commun. **19**, 359 (1998).
[7] M. Gerle, K. Fischer, A.H.E. Müller, M. Schmidt, S.S. Sheiko, S. Prokhorova, and M. Möller, Macromolecules **32**, 2629 (1999).
[8] K. Fischer and M. Schmidt, Macromol. Rapid Commun. **22**, 787 (2001).
[9] A. Gauger and T. Pakula, Macromolecules **28**, 190 (1995).
[10] Y. Rouault and O.V. Borisov, Macromolecules **29**, 2605 (1996).
[11] M. Saariaho, O. Ikkala, I. Szleifer, I. Erukhimovich, and G. ten Brinke, J. Chem. Phys. **107**, 3267 (1997).
[12] M. Saariaho, I. Szleifer, O. Ikkala, and G. ten Brinke, Macromol. Theory Simul. **7**, 211 (1998).
[13] Y. Rouault, Macromol. Theory Simul. **7**, 359 (1998).
[14] K. Shiokawa, K. Itoh, and N. Nemoto, J. Chem. Phys. **111**, 8165 (1999).
[15] A. Subbotin, M. Saariaho, O. Ikkala, and G. ten Brinke, Macromolecules **33**, 3447 (2000).
[16] A. Subbotin, M. Saariaho, R. Stepanyan, O. Ikkala, and G. ten Brinke, Macromolecules **33**, 6168 (2000).
[17] R.S. Ball, J.F. Marco, S.T. Milner, and T.A. Witten, Macromolecules **24**, 693 (1991).
[18] H. Lai and T.A. Witten, Macromolecules **27**, 449 (1994).
[19] L. Schäfer, *Excluded Volume Effects in Polymer Solutions* (Springer, Berlin, 1999).
[20] T.M. Birshtein, O.V. Borisov, E.B. Zhulina, A.R. Khokhlov, and T.A. Yurasova, Polym. Sci. U.S.S.R. **29**, 1293 (1987).
[21] G.H. Fredrickson, Macromolecules **26**, 2825 (1993).
[22] J.D. Cloizeaux, J. Phys. (Paris) **41**, 223 (1980).
[23] Y. Oono and T. Ohta, Phys. Lett. **85A**, 480 (1981).
[24] B. Duplantier, J. Phys. (Paris) **47**, 1633 (1986).
[25] M. Daoud and J.P. Cotton, J. Phys. (Paris) **43**, 531 (1982).
[26] K. Shiokawa, Polym. J. (Tokyo, Jpn.) **27**, 871 (1995).
[27] I. Wataoka, H. Urakawa, K. Kajiwara, M. Wintermantel, and M. Schmidt, Polym. Prepr. Jpn. **43**, 3571 (1994).